

# Macroscopic Volume Changes versus Changes of Free Volume As Determined by Positron Annihilation Spectroscopy for Polycarbonate and Polystyrene

J. Bohlen and R. Kirchheim\*

*Institut für Materialphysik, Universität Göttingen, Hospitalstr. 3-7, D-37073 Göttingen, Germany*

*Received July 24, 2000; Revised Manuscript Received January 25, 2001*

**ABSTRACT:** Positronium lifetimes in bisphenol A–polycarbonate (PC) and atactic polystyrene (PS) were measured as a function of temperature and hydrostatic pressure, and the results were compared with the macroscopic volume change of the polymer samples. A simple relation via the thermal expansion coefficient and the compressibility of the bulk material is applied and leads to direct information on the fractional free volume of the polymer in the investigated state and furthermore to the mean volume size of intermolecular holes. By plotting macroscopic volume changes vs changes of the hole volume as probed by the positronium, a linear relationship is obtained independent of whether the measurements were made above or below the glass transition temperature. The slope of the corresponding straight lines is steeper for samples exposed to hydrostatic pressure which is interpreted as a shrinkage of holes induced by pressure.

## Introduction

The microstructure of polymers in the molten or glassy state is of fundamental importance for the macroscopic behavior of polymer materials. The mechanical and viscoelastic behavior of a polymer is considered to be strongly dependent on the free volume. In addition, sorption of small molecules and their mobility depend on the size of intermolecular holes as described by free volume theories in the glassy states.<sup>1</sup> Many authors use orthopositronium (o-Ps) lifetimes as a measure of the size of the sites occupied by o-Ps; i.e., the holes are assumed to comprise part of the free volume between the macromolecules of the polymer.

In the framework of a simple quantum-mechanical model of o-Ps in a spherical hole, the lifetime was calculated to be<sup>2,3</sup>

$$\tau_{\text{o-Ps}} = \frac{1}{\Lambda[1 - R/(R + \Delta R) + 1/2\pi \sin(2\pi R/(R + \Delta R))]} \quad (1)$$

where  $R$  is the radius of the hole.  $\Lambda$  is an average decay rate of Ps which was estimated to be  $2 \text{ (ns)}^{-1}$ .  $\Delta R$  was determined to be  $1.66 \text{ \AA}$  by fitting data of molecular solids and zeolites with known hole sizes to eq 1. Radii calculated from measured lifetimes turn out to be much larger than those obtained from volume change caused by the sorption of small molecules like  $\text{CO}_2$  and others.<sup>1</sup> The holes as calculated from eq 1 are actually much larger than the volume of the dissolved molecules which should not lead to volume expansion during sorption in contradiction with experiment. Despite this disagreement, hole volumes obtained via eq 1 scale with macroscopic volume changes as observed during thermal expansion. Several measurements of o-Ps lifetimes in polymers as a function of temperature have been performed,<sup>4–6</sup> and all show that at the glass transition temperature the thermal expansion coefficient  $\alpha$  of the hole volume  $v_0$  as obtained from eq 1 changes similar to the behavior of the macroscopic volume  $V$ . A similar evaluation of pressure measurements is not known to

the best of our knowledge, and it will be a major goal of the present study to provide data of o-Ps lifetimes measured during pressurizing bisphenol A–polycarbonate (PC) and atactic polystyrene (PS). In addition, measurements were made as a function of temperature below and above the glass transition temperature. Results will be interpreted in terms of a simple free volume concept.

## Experimental Procedure

Bisphenol A–polycarbonate (PC) received from Bayer AG and atactic polystyrene (PS) received from BASF AG were investigated as a function of temperature and hydrostatic pressure. For temperature measurements films of about  $100 \text{ }\mu\text{m}$  thickness were prepared by drying a solution of the polymer in dichloromethane. A positron source of  $^{22}\text{NaCl}$  in aqueous solution was used. An amount corresponding to an activity of about  $1.5\text{--}3 \text{ MBq}$  was deposited onto the film over an area of  $15 \times 15 \text{ mm}^2$ , dried, and glued on top of another film by applying acetone. Therefore, an inner source within the material was realized. Samples were prepared by stacking several of these film pairs until a total thickness of  $4 \text{ mm}$  was reached. The package was placed in between two copper supports, and measurements were performed in a vacuum vessel with an internal furnace. Gas pressures between  $100 \text{ mPa}$  and  $1.5 \text{ MPa}$  can be realized within the chamber, and temperature was varied between  $295 \text{ K}$  (room temperature) and  $570 \text{ K}$ . To start with a well-defined sample state, measurements were performed by beginning at the highest temperatures well above the glass transition temperature  $T_g$ . Glass transition temperatures were determined to be  $420 \text{ K}$  for PC and  $377 \text{ K}$  for PS by differential scanning calorimetry (DSC) with a heating rate of  $20 \text{ K/min}$ .

A commercial injection valve for cars as produced by the BOSCH AG was used for measurements of polymers under compression. This enables a very close fit between piston and cylinder walls of the sample chamber. Cylindrical polymer samples were prepared by melting the granulated polymer within the valve. In between two of these cylindrical samples the positron source was placed the same way as described for the polymer films before. A compressive stress was applied on the two connected cylinders inside the valve with the aid of a commercial tensile testing machine which enabled us to measure the specific volume at the same time. The tempera-

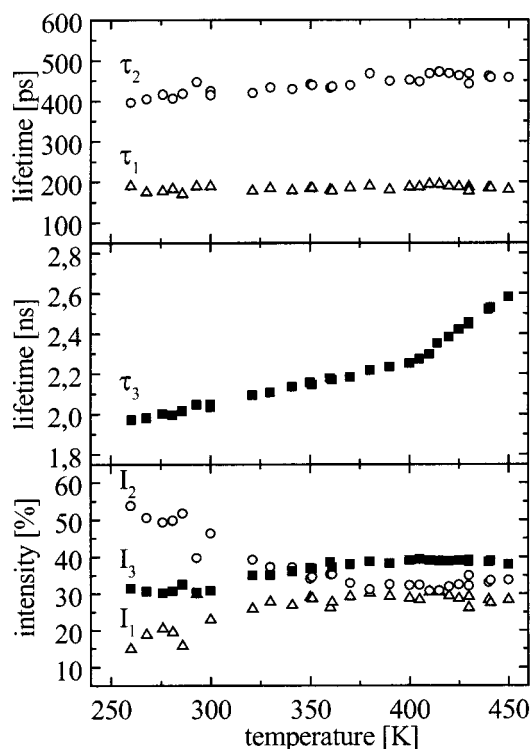


**Figure 1.** Lifetimes  $\tau_1$ ,  $\tau_2$ , and  $\tau_3$  as functions of temperature for PC. The relative intensities of the three components are shown in the lowest diagram.

ture during the experiment was held constant by a surrounding furnace.

For positron lifetime measurements two fast lifetime spectrometers were employed. Details of the setup and the measuring procedure are described elsewhere.<sup>7</sup> In all cases  $3 \times 10^6$  counts were collected for the lifetime spectra, yielding a time resolution of 180 and 200 ps fwhm. The program PATFIT was used to deconvolute the spectra. Best results were obtained by fitting the spectra with three free components. The longest one is of the order of a few nanoseconds, and therefore, it is attributed to the long-living o-Ps component. The two other components at around 200 and 500 ps are interpreted as the short-living parapositronium (p-Ps) component and a free positron component.

### Experimental Results

The measured spectra were evaluated with the program PATFIT, yielding independent of temperature and pressure almost the same values for the two short lifetimes whereas the o-Ps lifetime changed considerably. This is shown for two examples in Figures 1 and 2. In addition, the individual contribution of the three lifetimes to the total intensity did not vary much (cf. Figures 1 and 2). These two short lifetimes are of no interest in the framework of the present study because only the third one stemming from o-Ps provides reliable information about the hole volume. These values were inserted in eq 1 and from the evaluated radius  $R$  a hole volume  $v_0$  was calculated and plotted in Figures 3–7 for PC and PS as a function of temperature and pressure. In addition, the figures contain changes of the macroscopic specific volume  $V$  as obtained from ref 8 or as measured in this study.

In all cases linear changes of the macroscopic specific volume  $V$  of the two polymers are accompanied by corresponding increases or decreases of the microscopic volume  $v_0$ , respectively. Of course, the similar slopes for  $V$  and  $v_0$  in Figures 3–7 have no physical meaning as

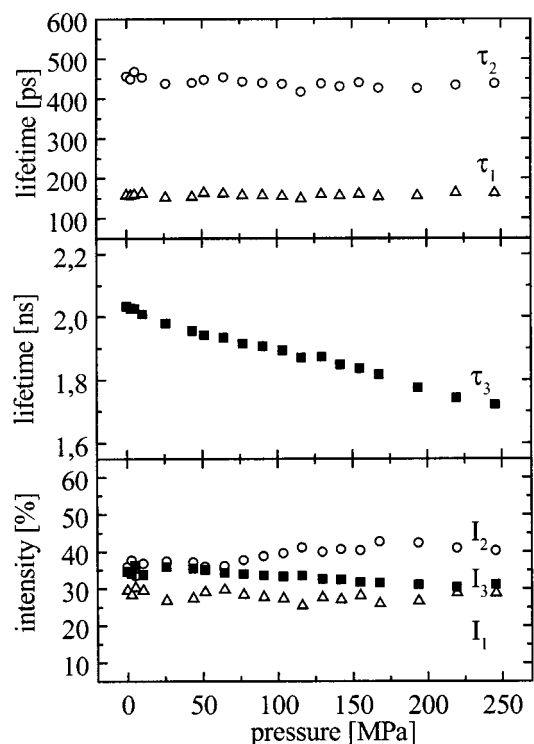


**Figure 2.** Lifetimes  $\tau_1$ ,  $\tau_2$ , and  $\tau_3$  as functions of hydrostatic pressure for PS. The relative intensities of the three components are shown in the lowest diagram.

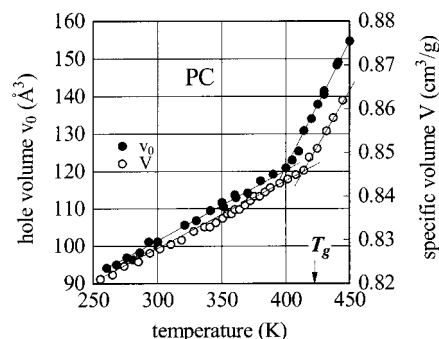


**Figure 3.** Hole volume  $v_0$  (full circles) in PC at ambient pressure (0.1 MPa) as obtained from o-Ps lifetimes and specific volume  $V$  (open circles) from ref 8 vs temperature. The measured calorimetric glass transition temperature  $T_g$  is shown for comparison.

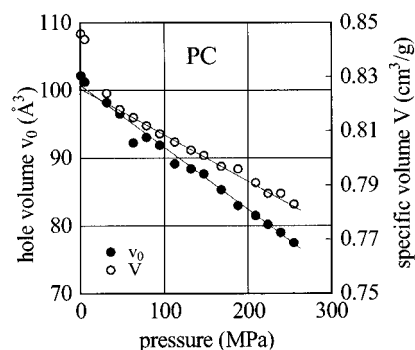


**Figure 4.** Hole volume  $v_0$  (full circles) in PC at 300 K as obtained from o-Ps lifetimes and specific volume  $V$  (open circles) as measured in this study vs compressive pressure.

they are a matter of scaling the corresponding axes. If a liquid/glass transition occurs, the slopes of straight lines corresponding to the linear relationship with either temperature (cf. Figures 3 and 4) or pressure (cf. Figure

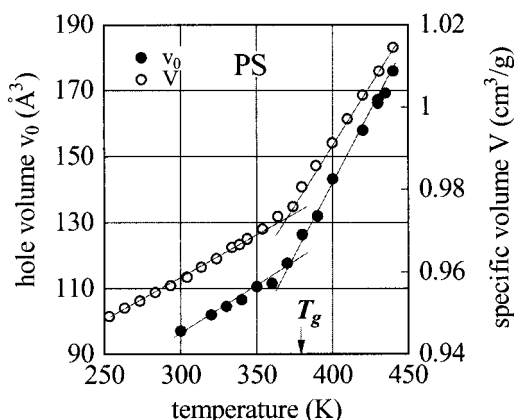


**Figure 5.** Hole volume  $v_0$  (full circles) in PS at ambient pressure (0.1 MPa) as obtained from o-Ps lifetimes and specific volume  $V$  (open circles) from ref 8 vs temperature. The measured calorimetric glass transition temperature  $T_g$  is shown for comparison.

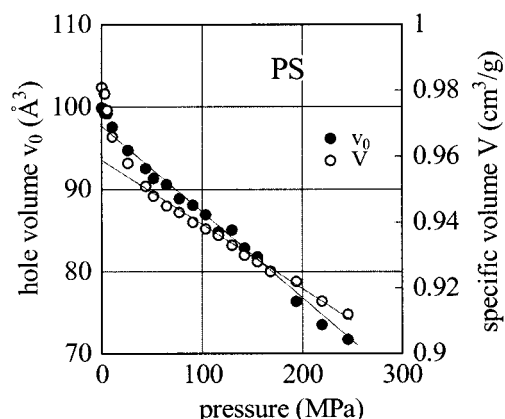


**Figure 6.** Hole volume  $v_0$  (full circles) in PS at 300 K as obtained from o-Ps lifetimes and specific volume  $V$  (open circles) as measured in this study vs compressive pressure.

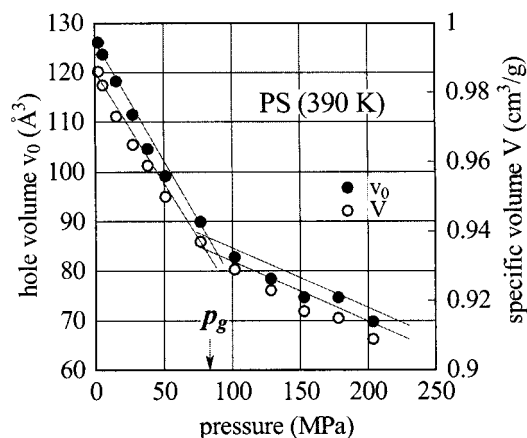


**Figure 7.** Hole volume  $v_0$  (full circles) in PS at 390 K as obtained from o-Ps lifetimes and specific volume  $V$  (open circles) as measured in this study vs compressive pressure. The pressure  $p_g$  where PS transforms into the glassy state is taken from ref 9 and shown for comparison.

7) change for both quantities  $V$  and  $v_0$ . The initial pressure values of  $V$  for both PC and PS are considered to be less reliable, because the piston and polymer sample within the pressure cell may have had bad contact in some areas at the beginning of the experiment.

The average compressibilities at 300 K obtained from Figures 4 and 6 are 5.8 GPa for PC and 5.4 GPa for PS in agreement with data from literature.<sup>10</sup> Glass transition temperatures as evaluated from the intersections of high- and low-temperature straight lines in Figures 3 and 5 are slightly smaller than the calorimetric ones determined for a heating rate of 20 K/min. This is in accordance with the glass transition temperature decreasing with decreasing heating rate because the measurements of a lifetime spectrum (a few hours per set temperature) or a dilatometric measurement correspond to slower heating rates.

## Discussion

To get some guidance in interpreting the hole volume data, we will discuss the specific volumes of polymers in the crystalline  $V_c$  and glassy state  $V_g$  in comparison with the van der Waals volume  $V_w$ . Although the two glassy polymers of this study do not crystallize, we will use the hypothetical crystalline state as a reference. In a compilation by Krevelen,<sup>10</sup> it is shown that the following relationships hold for a variety of polymers

$$V_c = 1.45 V_w \quad \text{and} \quad V_g = 1.60 V_w \quad (2)$$

Thus, the total intermolecular or empty volume is increased from 45% in a crystal to 60% in a glass and the relative difference between the two called excess volume  $V_e$  amounts to about 10%. The latter may be also determined from the density of the crystal as calculated from its structure and the macroscopic density of the glass. This has been done for the two polymers of this study, and the data are included in Table 1. The empty volume is usually separated into larger holes accessible for o-Ps and smaller entities according to the following relation:

$$V = V_w + V_{sm} + Nv_0 \quad (3)$$

where  $v_0$  is the average volume of the holes,  $N$  is their number per gram, and  $V_{sm}$  is the remaining specific free volume composed of small entities. It has been shown by computer simulations<sup>11</sup> very recently that within the distribution of hole sizes smaller and larger holes can be distinguished for polystyrene. The approach being the basis of eq 3 is analogous to the concept used in ref 12, if the fraction  $V_{sm}$  corresponds to non accessible holes either being too small or being blocked by fast vibrating segments.

It will be helpful to compare these considerations with crystalline materials composed of spherical building units, i.e., atoms. The relationship between the volume of the crystal and the van der Waals volume of its atoms is for the close packed fcc and hcp structure  $V_c = 1.35 V_w$ , for the less dense packed bcc structure  $V_c = 1.47 V_w$ , and for simple cubic lattices it is  $V_c = 1.92 V_w$ . Thus, by comparing with eq 2, we may state that we have a rather dense packing of the segments of a macromolecule within the crystalline state.

It is usually assumed that the excess volume of the glassy state and the fraction belonging to the larger holes are the same. Thus, the first two terms on the right-hand side of eq 3 are equivalent with  $V_c$ . Then the temperature and pressure dependence of the specific

**Table 1.** Density [g/cm<sup>3</sup>], Free Volume Fraction *f* As Defined by the Relative Difference of Molar Volumes between Glassy *V<sub>g</sub>* and Crystalline State *V<sub>c</sub>*,<sup>10</sup> and Slopes of the Linear Parts in Figures 3–7

	density [g/cm <sup>3</sup> ]	$f = (V_g - V_c)/V_g$ around 300 K	$dV/dT (T < T_g)$ [cm <sup>3</sup> /(g K)]	$dV/dT (T > T_g)$ [cm <sup>3</sup> /(g K)]	$dv_0/dT (T < T_g)$ [Å <sup>3</sup> /K]
PC	1.2	0.08	$1.5 \times 10^{-4}$	$5.3 \times 10^{-4}$	0.2
PS	1.05	0.1 (0.07)	$2.07 \times 10^{-4}$	$5.7 \times 10^{-4}$	0.27
	$dv_0/dT (T > T_g)$ [Å <sup>3</sup> /K]	$dV/dp (T < T_g)$ [cm <sup>3</sup> /(g K)]	$dv_0/dp (T < T_g)$ [Å <sup>3</sup> /MPa]	$dv_0/dp$ 390 K ( $p < p_g$ ) [Å <sup>3</sup> /MPa]	$dV/dp$ 390 K ( $p < p_g$ ) [cm <sup>3</sup> /MPa]
PC	0.69	$1.7 \times 10^{-4}$	0.094		
PS	0.81	$1.9 \times 10^{-4}$	0.11	0.55	$7.5 \times 10^{-4}$
	$dv_0/dp$ 390 K ( $p > p_g$ ) [Å <sup>3</sup> /MPa]	$dV/dp$ 390 K ( $p > p_g$ ) [cm <sup>3</sup> /MPa]	$N$ [g <sup>-1</sup> ] (from <i>T</i> )	$N = N_{eff}$ [g <sup>-1</sup> ] (from <i>p</i> )	$N = N_{eff}$ [g <sup>-1</sup> ] (from <i>p</i> ) 390 K
PC			$0.9 \times 10^{21}$	$2.3 \times 10^{21}$	
PS	0.13	$1.7 \times 10^{-4}$	$0.8 \times 10^{21}$	$2.0 \times 10^{21}$	$1.3 \times 10^{21}$

volume described by eq 3 are given by

$$\frac{\partial V_g}{\partial T} = \frac{\partial V_c}{\partial T} + \frac{\partial Nv_0}{\partial T} \quad \text{or} \quad \frac{\partial V_g}{\partial p} = \frac{\partial V_c}{\partial p} + \frac{\partial Nv_0}{\partial p} \quad (4)$$

The last equations can be rewritten in terms of a thermal expansion coefficient  $\alpha$  or an isothermal compressibility  $\kappa$ .

$$\alpha_g = \frac{1}{V_g} \frac{\partial V_g}{\partial T} = (1 - f) \frac{1}{V_c} \frac{\partial V_c}{\partial T} + f \frac{1}{Nv_0} \frac{\partial Nv_0}{\partial T} = (1 - f)\alpha_c + f\alpha_h \quad (5)$$

and

$$\kappa_g = \frac{1}{V_g} \frac{\partial V_g}{\partial p} = (1 - f) \frac{1}{V_c} \frac{\partial V_c}{\partial p} + f \frac{1}{Nv_0} \frac{\partial Nv_0}{\partial p} = (1 - f)\kappa_c + f\kappa_h \quad (6)$$

where  $f = Nv_0/V_g$  is the fraction of the accessible volume and  $\alpha_h$  and  $\kappa_h$  are the expansion coefficient and compressibility of holes as defined by the last two equations for constant values of *N*. Solving for *f* yields

$$f = \frac{\alpha_g - \alpha_c}{\alpha_h - \alpha_c} \quad \text{or} \quad f = \frac{\kappa_g - \kappa_c}{\kappa_h - \kappa_c} \quad (7)$$

As there are no single crystals of the two polymers used in this study, the determination of  $\alpha_c$  and  $\kappa_c$  is not possible. One may assume as in ref 4 that the lowest value of  $\alpha$  determined in the glassy state is equivalent with  $\alpha_c$ . In the case of PC this minimum value was measured in ref 4 to be  $1.11 \times 10^{-4} \text{ K}^{-1}$  for temperatures below the  $\gamma$ -relaxation. Thus, by definition, the free volume fraction *f* is zero at these low temperatures, which may be difficult to comprehend. On the other hand, expansion coefficients and compressibilities for the glassy polymers are rather large when compared with those for crystalline solids. This may be due to the overwhelming contribution from processes of segmental motion in the glass compared to the expansion caused by the anharmonicity of the atomic interaction potentials in a crystal. Therefore, we assume that both  $\alpha_c$  and  $\kappa_c$  are negligible in eq 7, and we obtain

$$f = \frac{\alpha_g}{\alpha_h} \quad \text{or} \quad f = \frac{\kappa_g}{\kappa_h} \quad (8)$$

This simple relationship is used in ref 12 as well as a

first-order approach called case I, although the separation of the total volume into various parts is somewhat different when compared with the present study.

Changes of both specific volume *V* and hole volume *v<sub>0</sub>* are found experimentally to be linear functions of pressure and temperature within both glassy and molten state. Corresponding slopes of the linear parts in Figures 3–7 are given in Table 1. Values of *f* obtained from eq 8 and data compiled in Table 1 are presented in Figures 8 and 9. Within the glassy state measurements of thermal expansion yield *f* values between 7 and 10% for PS and PC. These values are included in Table 1 and agree very well with those calculated from densities or molar volumes of the crystalline and glassy state according to eq 2 (cf. Table 1). Measurements of *o*-Ps lifetimes as a function of temperature below and above the glass transition temperature were made

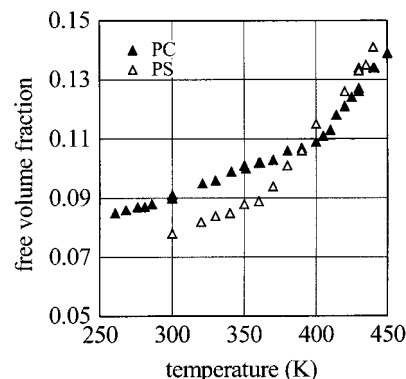


**Figure 8.** Free volume fraction as calculated by eq 5 and data from Figure 3 for PC (closed triangles) and Figure 5 for PS (open triangles) vs temperature.

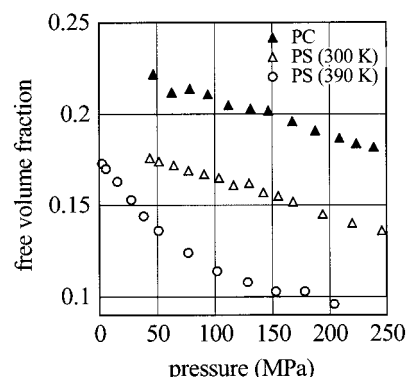


**Figure 9.** Free volume fraction as calculated by eq 6 and data from Figure 4 for PC (closed triangles) and Figure 6 for PS (open triangles) vs pressure.



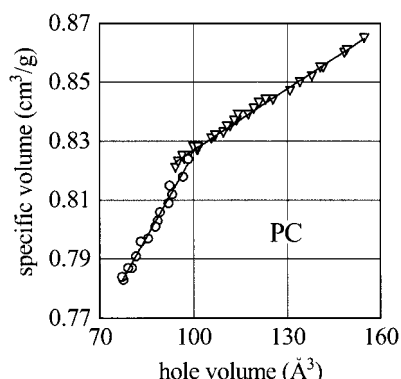


**Figure 10.** Macroscopic specific volume  $V$  as a function of microscopic hole volume  $v_0$  for PC and the data from Figures 3 (triangles) and 4 (circles).

before, and the values obtained in these studies<sup>4,12,13</sup> are in good agreement with the ones presented in Table 1.

According to the assumption made,  $f$  values represent the excess volume of the glassy state when compared with the crystalline one, and therefore, they do not include the intermolecular volume present in the crystalline state. The latter volume fraction is considered to consist of very small holes which most probably will not be visited by o-Ps. Free volume fractions  $f$  as obtained from measurements with varying pressure at 300 K (cf. Figure 9) are considerably larger than the ones obtained from temperature-dependent measurements. This may be due to a transformation of larger holes into smaller ones as discussed below.

By plotting the macroscopic volume  $V$  vs the microscopic one  $v_0$  as in Figures 10–12, the number of holes  $N$  is obtained from the slope of the straight parts according to eq 3. These  $N$  values are compiled in Table 1. In the following we will discuss three different aspects of the  $N$  values: (i) their magnitude, (ii) their continuity at the glass transition temperature or pressure, and (iii) their different values for pressure- and temperature-dependent experiments.

**Magnitude of  $N$  and  $v_0$  Values.** From the agreement between excess volume as calculated from densities and PLS data, one can conclude that the product  $Nv_0$  is correct. However, there are dilatometric data<sup>1</sup> using small molecules as probes of the hole size, stating that  $v_0$  is smaller by a factor of about 4. Occupying the larger holes by small molecules like CO<sub>2</sub> and Ar and determining the average volume of the remaining smaller holes by PLS<sup>7</sup> yields values of  $N$  which are larger by a factor of 4. Thus, the product  $Nv_0$  becomes the same. Assuming that the average hole volume of about 100 Å<sup>3</sup> as obtained from PLS is correct leads to a disagreement with volume expansions observed for the dissolution of small molecules within the holes; i.e., CO<sub>2</sub> having a volume of about 77 Å<sup>3</sup> causes a volume increase of about 20 Å<sup>3</sup>. We will not extend this discussion because both approaches PLS and molecules as probe use several simplifying assumptions which may cause systematic errors. To state it positively, both very different approaches yield values of the same order of magnitude.

**Continuity of  $N$  Values at the Glass Transition.** Although the thermal expansion coefficient and the compressibility show a discontinuity at the glass transition temperature, the hole density value  $N$ , as the slope of the curves in Figures 10–12, does not. Therefore, the increased thermal expansion of the total volume and of

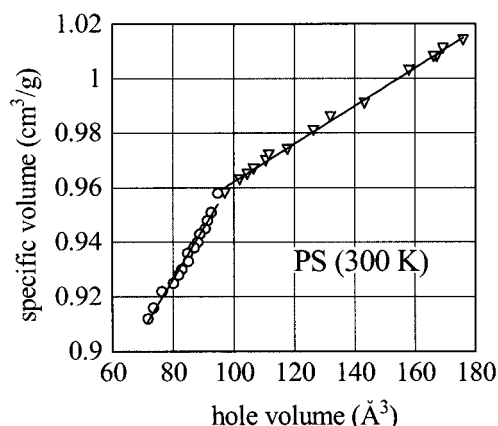


**Figure 11.** Macroscopic specific volume  $V$  as a function of microscopic hole volume  $v_0$  for PS and the data from Figures 5 (triangles) and 6 (circles).

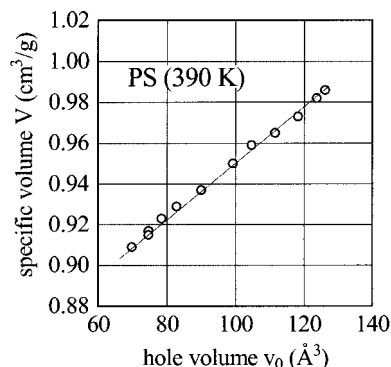


**Figure 12.** Macroscopic specific volume  $V$  as a function of microscopic hole volume  $v_0$  for PS and the data from Figure 7.

the holes above  $T_g$  is not due to the creation of new holes but has to be attributed to an increase of the dynamics of the reorientation of molecular groups within the polymer.

**Transformation of Large to Small Holes by Hydrostatic Pressure.** In the following we propose an explanation for the changing slope in Figures 10 and 11 by going from thermal expansion data to pressure data. The latter exhibit a larger slope which corresponds to a larger hole density (cf. Table 1). The pressures applied are well above the flow stresses in compression tests, and one may assume that flow occurs within the confined samples as well on a microscopic level. This is described by a simple reaction



where large holes of volume  $v_{lh}$  transform to small holes of volume  $v_{sh}$ , and vice versa. The small holes shall further on belong to the excess volume, and therefore, different than the even smaller holes in the crystalline states, they shall be occupied by o-Ps. To relate this approach to a more realistic distribution of hole volumes with average value  $v_0$  and width  $\sigma_v$ , we use a Gaussian distribution which is degenerated into two discrete volumes. The small ones may be all those with  $v_{lh} < v_0$  and vice versa for the larger ones. Calculating the average values of hole volumes for these two parts of the Gaussian yields  $v_{sh} = v_0 - \sigma_v/\sqrt{\pi}$  and  $v_{lh} = v_0 + \sigma_v/\sqrt{\pi}$  and a difference of  $\delta v = v_{lh} - v_{sh} = 2\sigma_v/\sqrt{\pi}$ .

The corresponding rate equations for eq 9 are

$$\frac{dN_l}{dt} = -\frac{dN_s}{dt} = -k_-N_l + k_+N_s \quad (10)$$

where  $N_i$  are the number densities of small or large holes and the rate constants  $k_+$  and  $k_-$  depend on pressure according to the volume change  $\delta v = v_{lh} - v_{sh}$

$$k_{\pm} = k_0 \exp\left(\mp \frac{p\delta v}{RT}\right) \quad (11)$$

For zero pressure we have in agreement with the definition of small and large holes

$$N_l = N_s = \frac{N}{2} \quad (12)$$

For steady-state conditions  $dN_i/dt = 0$  and nonzero pressure eq 11 gives

$$\frac{N_l}{N_s} = \exp\left(-\frac{2p\delta v}{RT}\right) \approx 1 - \frac{2p\delta v}{RT} \quad (13)$$

where it has been assumed that  $2p\delta v \ll RT$  to linearize the exponential. Of course, this will be true for small pressures only.

Using the following definition for  $\Delta N$

$$N_l = \frac{N}{2} - \Delta N \quad \text{and} \quad N_s = \frac{N}{2} + \Delta N \quad (14)$$

eq 13 can be expressed as

$$\frac{N_l}{N_s} = \frac{N - 2\Delta N}{N + 2\Delta N} = \left(1 - \frac{2p\delta v}{RT}\right) \quad (15)$$

With the additional assumption of small changes, i.e.,  $\Delta N \ll N$  the last equation becomes

$$\frac{\Delta N}{N} = \frac{p\delta v}{2RT} = \frac{p\sigma_v}{RT\sqrt{\pi}} \quad (16)$$

The macroscopic volume change of a sample  $\Delta V$  then contains a contribution from the continuous change of the hole volume,  $N\Delta v_h$ , and a discontinuous one according to eq 9,  $\Delta N\delta v = \Delta N2\sigma_v/\sqrt{\pi}$ .

$$\Delta V = N\Delta v_h + \frac{\Delta N2\sigma_v}{\sqrt{\pi}} = N\Delta v_h + \frac{Np4\sigma_v^2}{\pi RT} = N\Delta v_h \left(1 + \frac{4C\sigma_v^2}{\pi RT}\right) \quad (17)$$

where  $C$  is the proportionality constant for the experimentally observed relation  $p \propto \Delta v_h$ . Thus, the slope  $\Delta V/\Delta v_h$  in Figures 10–12 corresponds to an effective hole number density defined as

$$N_{\text{eff}} = N \left(1 + \frac{4C\sigma_v^2}{\pi RT}\right) \quad (18)$$

which is larger than  $N$  in agreement with experimental findings. Using values for the width of the Gaussian distribution as obtained from PLS data,  $\sigma_v = 1.2 \times 10^{-5} \text{ m}^3/\text{mol}$  for PC<sup>14</sup> and  $\sigma_v = 1.2 \times 10^{-5} \text{ m}^3/\text{mol}$  for PS,<sup>15</sup> and data from this study,  $C = 1.8 \times 10^{13} (\text{mol N})/\text{m}^5$  for PC and  $C = 1.5 \times 10^{13} (\text{mol N})/\text{m}^5$  for PS (cf. Table 1), the following relations are calculated

$$N_{\text{eff}} = 2.3N \text{ for PC} \quad \text{and} \quad N_{\text{eff}} = 2.1N \text{ for PS} \quad (19)$$

which are in very good agreement with the values presented in Table 1.

In agreement with experimental data at 390 K for PS, eq 18 predicts that the effective number density  $N_{\text{eff}}$  is smaller at higher temperatures. However, the quantitative dependence on temperature is much stronger for the experimental results. This may be due to errors in  $\sigma_v$  values and errors caused by the expansion of the exponential in eq 13 and due to deviations from the steady-state condition  $dN/dt = 0$ . Choosing a distribution of hole volumes which is different from the Gaussian one should not affect the results very much; i.e., a box-type distribution gives rise to  $\delta v = v_{lh} - v_{sh} = 2\sigma_v/2$  instead of  $\delta v = v_{lh} - v_{sh} = 2\sigma_v/\sqrt{\pi}$ .

**Acknowledgment.** The authors are grateful for the assistance provided by Prof. Th. Hehenkamp and co-workers, who allowed us to use their experimental equipment. We also thank the Deutsche Forschungsgemeinschaft for financial support.

## References and Notes

- (1) Gotthardt, P.; Gröger, A.; Brion, H. G.; Plaetschke, R.; Kirchheim, R. *Macromolecules* **1997**, *30*, 8058.
- (2) Tao, S. J. *J. Chem. Phys.* **1972**, *56*, 5499.
- (3) Jean, Y. C. *Microchem. J.* **1990**, *42*, 72.
- (4) Kristiak, J.; Bartos, J.; Kristiakova, K.; Sausa, O.; Bandzuch, P. *Phys. Rev. B* **1994**, *49*, 6601.
- (5) Kluin, J. E.; Yu, Z.; Vleeshouwers, S.; McGervey, J. D.; Jamieson, A. M.; Simha, R.; Sommer, K. *Macromolecules* **1993**, *26*, 1853.
- (6) Dlubek, G.; Saarinen, K.; Fretwell, H. M. *J. Polym. Sci., Part B: Polym. Phys.* **1998**, *36*, 1513.
- (7) Bohlen, J.; Wolff, J.; Kirchheim, R. *Macromolecules* **1999**, *32*, 3766.
- (8) Greiner, R.; Schwarzl, F. R. *Rheol. Acta* **1984**, *23*, 378.
- (9) Rehage, G.; Breuer, H. *J. Polym. Sci., Part C* **1967**, *16*, 2299.
- (10) Van Krevelen, D. W. *Properties of Polymers*; Elsevier: Amsterdam, 1990; pp 71ff and 790.
- (11) Schmitz, H.; Müller-Plathe, F. *J. Chem. Phys.* **2000**, *112*, 1040.
- (12) Hristov, H. A.; Bolan, B.; Yee, A. F.; Xie, L.; Gidley, D. W. *Macromolecules* **1996**, *29*, 8507.
- (13) Sndreczki, T. C.; Hong, X.; Jean, Y. C. *Macromolecules* **1996**, *29*, 4015.
- (14) Jean, Y. C.; Yuan, J.-P.; Liu, J.; Deng, Q.; Yang, H. *J. Polym. Sci., Part B: Polym. Phys.* **1995**, *33*, 2365.
- (15) Liu, J.; Deng, Q.; Jean, Y. C. *Macromolecules* **1993**, *26*, 7149.

MA0012970